Josephson junction with current in a strong magnetic field

G. F. Zharkov

P.N. Lebedev Physics Institute, USSR Academy of Sciences
(Submitted 22 May 1978)
Zh. Eksp. Teor.Fiz. **75**, 2196–2209 (December 1978)

The behavior of a current-carrying Josephson junction of finite width placed in a strong magnetic field H_e is considered. In contrast to the earlier studies of this subject, where numerical methods were used, the nonlinear equation is investigated analytically. All the possible solutions of the corresponding boundary-value problem are analyzed and are checked for stability. It is shown that stable and unstable field and current configurations exist in the junction and correspond to a distributed vortex structure; a criterion for the stability of the solution is indicated. It is shown that the dependence of the maximum current through the junction on the external magnetic field $I_{max}\sim(\sin\phi)/\phi$ ($\phi = H_eL/2$), previously obtained from simple physical considerations for junctions of small width L, remain in force in a strong field also for junctions of finite width. The existence of a unique "geometric resonance," is indicated, wherein junctions that differ in width by $2\pi/H_e$ (in dimensionless units) must simultaneously go over to a nonstationary regime when equal currents are made to flow through them.

PACS numbers: 74.50. + r.

1. INTRODUCTION

Josephson tunnel junctions are extensively used in modern devices intended for precision measurements of magnetic fields (the so-called SQUID quantum interferometers, see, e.g., Refs. 1 and 2), as well as for other purposes. It is therefore of both theoretical and practical interest to describe the physical processes that occur in tunnel junctions. This paper deals with the behavior of a Josephson junction of finite width L, placed in an external magnetic field H_e and carrying a transport current I. This problem was previously considered by numerical methods by Owen and Scalapino.[3] It is shown below that this problem admits of an analytic description in the limiting case of a strong external field.

The initial equation that describes the stationary distribution of the field and of the current in a Josephson junction is[1,2]

$$d^2\varphi/dx^2=\sin\varphi(x). \tag{1}$$

The quantity $\varphi(x)$ (called the phase difference of superconductor wave functions) is connected with the magnetic field in the junction

$$d\varphi/dx=H(x). \tag{2}$$

Dimensionless unit are used in Eqs. (1) and (2) (see Refs. 1 and 2).

We consider a one-dimensional problem, where current flows along the z axis (see Fig. 1), the external magnetic field is perpendicular to the plane of the figure and is directed along the y axis, and the distribution of the field and the current in the barrier depend only on a single coordinate x. The boundary conditions for this problem are

$$\left.\frac{d\varphi}{dx}\right|_{x=0}=H_0, \quad \left.\frac{d\varphi}{dx}\right|_{x=L}=H_L, \tag{3}$$

with

$$H_0=H_e-H_I, \quad H_L=H_e+H_I, \tag{4}$$

where H_e is the external magnetic field and H_I is the intrinsic magnetic field due to the transport current flowing through the junction, $I=2H_I$.

We note that the boundary-value problem (3) for Eq. (1) is not unique: given H_0 and H_L, several solutions satisfy the conditions (3). It is therefore convenient to formulate[4-7] in place of (3) the equivalent Cauchy problem

$$\varphi|_{x=0}=\varphi(0), \quad \left.\frac{d\varphi}{dx}\right|_{x=0}=H_0, \tag{5}$$

where $\varphi(0)$ is the value of the function φ at $x=0$. Since the Cauchy problem defines uniquely the solution of the differential equation, reduction of the boundary-value problem (3) to the Cauchy problem (5) is convenient in the analysis of (1).

We obtain below the value of $\varphi(0)$ as a function of the parameters of the boundary-value problem (L, H_0, H_L). The solution obtained with the aid of Cauchy problem (5) will then automatically satisfy the conditions (3).

Equation (1) has a first integral in the form

$$x=\frac{1}{2}\int_{\varphi(0)}^{\varphi(x)}\frac{dy}{R(y)}, \quad R(y)=\left\{\sin^2\frac{y}{2}+C\right\}^{1/2}, \tag{6}$$

where C is an arbitrary integration constant, with

$$H(x)=2\{\sin^2(\varphi(x)/2)+C\}^{1/2}. \tag{7}$$

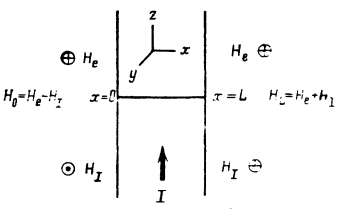

FIG. 1. Junction in an external field.

 0038-5646/78/1201107-07$02.40

From the conditions (3) we have

$$C=H_0^2/4-\sin^2(\varphi(0)/2)=H_L^2/4-\sin^2(\varphi(L)/2). \quad (8)$$

This yields the value of $\varphi(L)$:

$$\varphi(L)=\pm 2A+2\pi n, \quad A=\arcsin\{H_eH_I+\sin^2(\varphi(0)/2)\}^{1/2}. \quad (9)$$

We have chosen here for A the principal value of the arcsine: $0\leq A\leq\pi/2$.

Substituting $x=L$ in (6) and using (9), we obtain an integral equation for $\varphi(0)$:

$$L=\frac{1}{2}\int_{\varphi(0)}^{\pm 2A+2\pi n}\frac{dy}{R(y)}, \quad R(y)=\left\{\frac{H_0^2}{4}+\sin^2\frac{y}{2}-\sin^2\frac{\varphi(0)}{2}\right\}^{1/2}. \quad (10)$$

We note that the solutions of (1) are defined only in modulo 2π, i.e., it is always possible to add the solution the number $2\pi n$, where n is an integer. Using this circumstance, we can assume that $\varphi(0)$ lies in the interval $-\pi\leq\varphi(0)\leq\pi$. We consider separately the solution branches that begin with the values $\varphi(0)<0$ and $\varphi(0)>0$.

2. CLASSIFICATION OF THE SOLUTIONS AND REGIONS OF THEIR EXISTENCE

In the general case, the elliptic integral in (10) cannot be calculated analytically and the problem calls for numerical calculations. In the case of strong external fields ($H_e\gg 1$), however, this integral degenerates and Eq. (10) reduces to

$$H_eL=\pm 2A\pm|\varphi(0)|+2\pi n, \quad (11)$$

where A is defined in (9). In accordance with the four possible combination of the plus and minus signs in (11), we have four equations that define four types of solution[1)] of the initial equation (1).

These equations can be written in the form

$$\begin{aligned}
&\phi=n\pi-\xi+A(\xi)=J_{4n}(\xi), && (^1/_2\varphi(L)=A(\xi)+n\pi),\\
&\phi=n\pi+\xi+A(\xi)=J_{4n+1}(\xi), && (^1/_2\varphi(L)=A(\xi)+n\pi),\\
&\phi=(n+1)\pi-\xi-A(\xi)=J_{4n+2}(\xi), && (^1/_2\varphi(L)=\pi-A(\xi)+n\pi),\\
&\phi=(n+1)\pi+\xi-A(\xi)=J_{4n+3}(\xi) && (^1/_2\varphi(L)=\pi-A(\xi)+n\pi),
\end{aligned} \quad (12)$$

where $A(\xi)=\arcsin\{H_eH_I+\sin^2\xi\}^{1/2}$ and we have put $\xi=\frac{1}{2}|\varphi(0)|$ $(0\leq\xi\leq\pi/2)$, $\phi=\frac{1}{2}LH_e$, and $n=0,1,2,\ldots$. In the parentheses on the right sides of (12) are indicated the values of $\varphi(L)$ for the corresponding solutions, obtained in accordance with (9). The functions $J_N(\xi)$ are shown in Fig. 2a for $n=0,1,2$. They are integral curves [see (10)], and the points of intersection ξ_N of these curves with the horizontal line $J=\phi$ correspond to different roots of Eqs. (12). Each root gives the possible initial values of the function $\varphi(0)=\pm 2\xi_N$ that enters in the Cauchy problem (5), and determines uniquely the corresponding solution $\varphi_N(x)$. Knowledge of the number of the solution and of the position of the representative point on the curves of Fig. 2a serve as the basis for the classification of all the possible solutions of the problem (1)–(3). (The explicit form of the solutions $\varphi_N(x)$ is given in Sec. 4 below and is illustrated in Figs. 5 and 6.)

As is clear from Fig. 2a, the roots of Eq. (12) exist only in definite intervals of the values of $\phi=LH_e/2$.

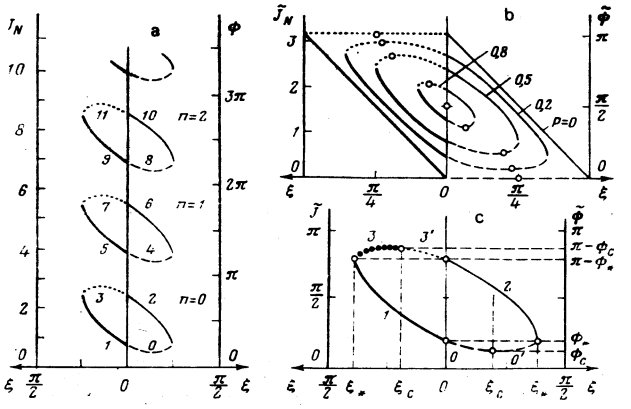

FIG. 2. Integral curves (12) as functions of the parameter ξ. The numbers on the curves correspond to the number of the solution. a) Curves at $p=H_eH_I=0.5$. The intersection of the curves with the horizontal line $J=\phi$ yields the initial value $|\varphi(0)|=2\xi_N$. b) Family of reduced curves ($J=J-n\pi$, $\tilde\phi=\phi-n\pi$, $\phi=H_eL/2$ at $p=0$, 0.2, 0.5, and 0.8). The light circles show the extremal points of the curves. c) Characteristic points of curves; their designations are given on the axes. The thick sections of the curves correspond to stable solutions. (One of the curves at $n=0$ is shown, the numbers on the curves correspond to the number of the solution, the light circles separate different types of solutions).

Introducing the notation $J_N=J_N-n\pi$, $\phi=\phi-n\pi$, we can refer all the J_N curves corresponding to different n (see Figs. 2a) to a single quadrant $-\pi/2\leq\xi\leq\pi/2$, $0\leq\tilde\phi\leq\pi$ (see Fig. 2b, which shows curves corresponding to different values of the parameter $p=H_eH_I$). The roots for the values $\phi=\tilde\phi+n\pi>\pi$ coincide with the corresponding values of the roots in the interval $0\leq\phi\leq\pi$. Figure 2c shows one of the curves of the family of Figs. 2b, on which the characteristic points are separated. The light circles in Figs. 2b and 2c show the extremum points of the functions J_0 and J_3 (as well as of all the functions J_{4n} and J_{4n+3}). It is seen, for example, that at a given ϕ there exists two different roots of the equations $\phi=J_0$, which determine different solutions of the problem (to distinguish between these solutions, one of the branches on Fig. 2b is labeled with a primed number: $N=0$ and $N=0'$; the same situation holds for the solutions $N=3$ and $N=3'$ and analogously for all the solutions $N=4n$ and $N=4n+3$). It will be shown below (see Sec. 5) that points lying on the branches of curves 0, 1, and 3 determine stable solutions of the problem (these branches are shown in Fig. 2c by thick curves). On the other hand, points lying on branches 0′, 2, and 3′ correspond to stable solutions (they are shown by thin lines). The points of all J_N curves on Figs. 2a and 2b are classified in the same manner.

Those roots of Eqs. (12) which determine the initial values of the Cauchy problem can be obtained in explicit form:

$$\begin{aligned}
&\xi_{4n}=-^1/_2\tilde\phi+^1/_2a(\phi), && \xi_{(4n)'}=^1/_2\pi-^1/_2\tilde\phi-^1/_2a(\phi),\\
&&& \phi_c\leq\tilde\phi\leq\phi_*;\\
&\xi_{4n+1}=^1/_2\tilde\phi-^1/_2a(\phi), && \xi_{4n+2}=^1/_2\pi-^1/_2\tilde\phi-^1/_2a(\phi),\\
&&& \phi_*\leq\tilde\phi\leq\pi-\phi_*;\\
&\xi_{4n+3}=^1/_2\tilde\phi-^1/_2a(\phi), && \xi_{(4n+3)'}=-^1/_2\pi+^1/_2\tilde\phi+^1/_2a(\phi),\\
&&& \pi-\phi_*\leq\tilde\phi\leq\pi-\phi_c.
\end{aligned} \quad (13)$$

We have put here $\tilde{\phi}=\phi-n\pi$ (the quantity $\tilde{\phi}$ lies inside the interval $0<\tilde{\phi}<<\pi$, and the symbols ϕ_* and ϕ_c are defined below),

$$a(\phi)=\arcsin\frac{H_eH_I}{|\sin\phi|}\leqslant\frac{\pi}{2}. \tag{14}$$

Under each formula is (13) is indicated the field interval ($\phi=H_eL/2$) in which the roots (13) exist. Obviously, the limits of the existence of the solutions coincide with the extremum points of the function $J_{4n}(\xi)$ and $J_{4n+3}(\xi)$ (see Fig. 2a). In accordance with (12), the $J_{4n}(\xi)$ curves have a minimum at the point $\xi=\xi_c$, where

$$\xi_c=\arcsin\{(1-H_eH_I)/2\}^{1/2}, \tag{15}$$

and the curves $J_{4n+3}(\xi)$ have maxima at the point $\xi=\xi_c$. From this, in particular, we obtain the value of $\phi_c=J_0(\xi_c)$:

$$\phi_c=\arcsin H_eH_I, \tag{16}$$

corresponding to the minimum of the $J_0(\xi)$ curve [see Fig. 2c and formulas (12)], and the value $\phi=\pi-\phi_c$ corresponding to the maximum of the $J_3(3)$ curve.

It is also possible to find the value $\xi=\xi_*$ at which the branches of the curves 0′ and 2 on Fig. 2c terminate, and the corresponding values of $\phi_*=J_0(\xi=\xi_*)$, namely

$$\begin{aligned}\xi_*&=\arcsin\{1-H_eH_I\}^{1/2},\\ \phi_*&=\arcsin(H_eH_I)^{1/2}.\end{aligned} \tag{17}$$

We note that $J_1(\xi=0)=J_{0'}(\xi=\xi_*)$ (see Fig. 2c). The locations of the remaining characteristic points for the $J_N(\xi)$ curves is clear from Fig. 2c.

As seen from Fig. 2a, with increasing parameter $\phi=H_eL/2$ (at a given value of H_I), the point of intersection of the $J_N(\xi)$ curves with the horizontal line $J_N=\phi$ that represents the static solution of the problem shifts along the corresponding curve, reaches the point of the maximum of the curve, and enters the forbidden region, where there are not static solutions. In this region, consequently, a nonstationary regime is realized. With further increase of ϕ the representative points lands on the lower branches of the J_N curves, corresponding to static solutions, etc. The field intervals in which static solutions exist can be represented in the form

$$\phi_c+n\pi\leqslant\phi\leqslant\pi-\phi_c+n\pi,\quad n=0,\ 1,\ 2,\ \dots, \tag{18}$$

or $\phi_c\leqslant\phi\leqslant\pi-\phi_c(\tilde{\phi}=\phi-n\pi<\pi)$, as written in (13).

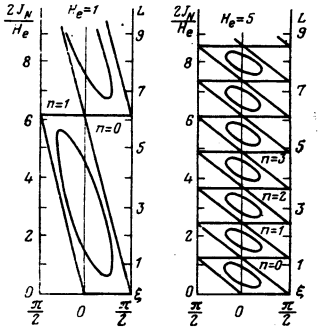

FIG. 3. Transformation of the integral curves with variation of the parameter H_e but at fixed values of $j_L=2H_I/L$.

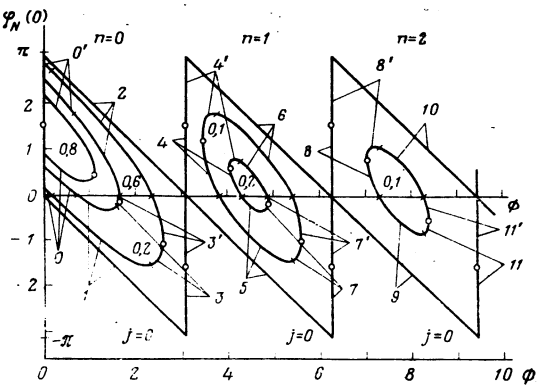

FIG. 4. Plots of $\varphi_N(0)$ against $\phi=H_eL/2$, obtained from formulas (13) at several values of the parameter $j_L=2H_I/L$ ($j_L=0$, 0.1, 0.2, 0.6, and 0.8, see the numbers on the curves). The light circles denotes the termination points of the static solutions. The indicated numbers of the solutions correspond to different sections of the curves.

Figure 3 shows the transformation of the integral curves $J_N(\xi)$ with changing parameter H_e but at a fixed value of H_I, while Fig. 4 shows the functions $\varphi_N(0)$ obtained from formulas (13) for $L=1$ and for several values of H_I.

3. EXPLICIT FORM OF THE SOLUTIONS AT $H_e\gg1$

Knowing the initial value of the function $\varphi_0=\varphi(0)$, we can construct the concrete solution $\varphi(x)$ of Eqs. (1), satisfying the conditions (3) or (5). In the general case the solution of Eq. (1) is expressed in terms of Jocobi elliptic functions. In the case $H_e\gg1$, the solution simplifies and can be expressed in terms of elementary functions. Using the expansion of expressions (6)–(8) at $H_e\gg1$ ($H_0\gg1$) or directly from Eq. (1) we obtain an approximate solution for $\varphi(x)$:

$$\varphi(x)=\varphi_0+H_0x+\left\{\frac{\cos\varphi_0}{H_0}x-\frac{1}{H_0^2}[\sin(\varphi_0+H_0x)-\sin\varphi_0]\right\}, \tag{19}$$

with

$$\frac{d\varphi}{dx}=H_0+\left\{\frac{\cos\varphi_0}{H_0}-\frac{\cos(\varphi_0+H_0x)}{H_0}\right\},\quad \frac{d^2\varphi}{dx^2}=\sin(\varphi_0+H_0x). \tag{20}$$

The solution (19) satisfies the initial conditions (5), and at $x=L$ we get

$$\left.\frac{d\varphi}{dx}\right|_{x=L}=H_L=H_0+\left\{\frac{\cos\varphi_0}{H_0}-\frac{\cos(\varphi_0+H_0L)}{H_0}\right\}. \tag{21}$$

Taking relations (4) into account, we can rewrite (21) in the form

$$H_0H_I=\sin^2(\varphi_L/2)-\sin^2(\varphi_0/2),\quad \varphi_L=\varphi_0+H_0L,$$

or

$$\varphi_L=\pm2\arcsin\{H_0H_I+\sin^2(\varphi_0/2)\}^{1/2}+2\pi n. \tag{22}$$

The condition (22) at $H_e\gg1$ is equivalent to the exact relation (9). Thus, examination of the approximate solution (19) led us again to the need for analyzing four possible types of solutions of Eq. (22) [or (9)], i.e., we arrive again at the problem considered in the preceding sections.

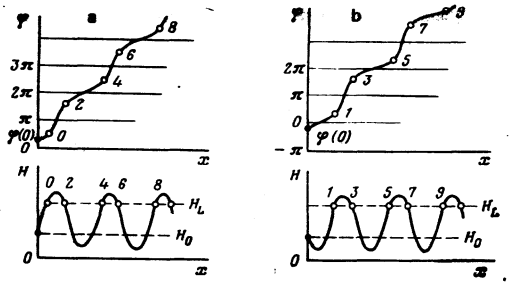

FIG. 5. General form of the solutions $\varphi(x)$ and of the field distributions $H(x)$ (schematic). The numbers of the curves correspond to the numbers of the corresponding solution (for example, the solution $N=2$ corresponds to the section of the curve from the point $\varphi(0)$ to the point 2). Two branches of the curves, beginning with $\varphi(0)>0$ (a) and with $\varphi(0)<0$ (b) are shown.

We note that formulas (19)–(21) yield a self-consistent solution of the problem only if account is taken of the small nonlinear term in the curly brackets. If this term is disregarded (linear approximation, $\varphi=\varphi_0+H_0x$) we have $d^2\varphi/dx^2=0$ in contradiction to the initial equation (1), and are unable to introduce the transport current I into the problem, since we get $H_0=H_L$, i.e., $I=0$. Obviously, it is precisely this small nonlinear term which takes into account the fact that new solutions vanish and appear, and determines the regions of their existence, i.e., characterizes the bifurcation points of Eq. (1) (see Ref. 8). When this term is neglected, the solution loses all its nonlinear properties.

Figure 5 shows schematically the general form of the solutions and indicates separately the branches that start from $\varphi(0)>0$ and $\varphi(0)<0$. From the form of the field distribution $H(x)$ it is clear that the numbers of the field extrema of neighboring solutions (0 and 2, 1 and 3, etc.) differ by unity. The field extrema coincide with the points $\varphi=n\pi$ [see (7)]; at these points $j(x)=\sin\varphi(x)=0$, i.e., they constitute centers of vortex currents in the junction (the currents are oppositely directed on the two sides of these points). The number of extremal points of solutions whose number n differs by unity (0 and 4, 1 and 5, etc.) differ by two, and accordingly they contain different numbers of vortices.

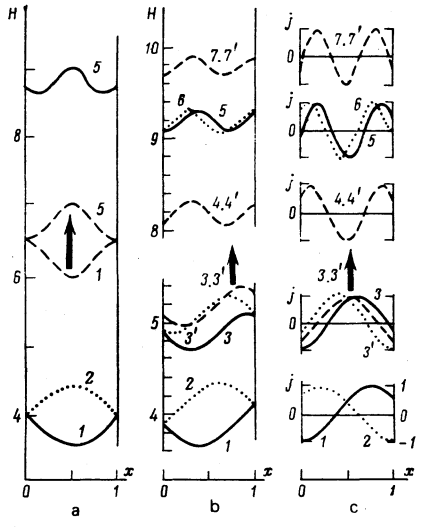

FIG. 6. Change of the distribution of the field (a and b) and of the current (c) in a barrier with $L=1$ with increasing external H_e ($H_0=H_e-H_1$, for $j_L=2H_1/L=0$ (a) and $j_L=0.2$ (b and c). Solid curves—stable solutions, dotted lines—unstable, dashed—curves corresponding to the stability limit. The arrow marks the onset of the nonstationary behavior and the transition from branch to branch.

Figure 6 shows the variation of the distribution of the current and of the field in a junction with $L=1$ with increasing external field [see formulas (19) and (20)]. The dashed curves show the distribution on the stability boundary, where a nonstationary transition takes place from one branch of the solution to another (the transitions are indicated by thick arrows). We note that even in the absence of a transport current ($H_I=0$, Fig. 6a), stability is lost at certain points and nonstationary transformation of the solutions takes place (for example, solution 1 is transformed into solution 5; more details of the character of the time evolution of the solutions are given in Refs. 5–7). Thus, in the absence of a transport current, the vortices enter the junction jumpwise. In the presence of a transport current (Figs. 6d and 6c) there exists a certain field interval wherein an extremal point appears inside the junction near one of its edges, and the stability is not lost thereby (for example, the solution 1 is gradually transformed into solution 3, for which there is a zero of the current, i.e., an extremum of the field) on the right-hand edge of the junction. These solutions corespond, in accord with the terminology adopted in Refs. 3 and 2, to solutions with an intermediate number of vortices. With further increase of the field, the transition is first into a nonstationary regime, after which the stationary region is again reached (see also Sec. 5).

4. INVESTIGATION OF THE STABILITY OF THE SOLUTIONS

The investigation of the stability of the solutions of Eq. (1) will be checked by a scheme already used by us earlier.[5-7] We consider in place of (1) the more general time-dependent equation[1,2]

$$\frac{\partial^2\varphi}{\partial t^2}+\beta\frac{\partial\varphi}{\partial t}-\frac{\partial^2\varphi}{\partial x^2}+\sin\varphi=0, \tag{23}$$

where t is the dimensionless time and β is phenomenological parameter that takes into account the damping of the temporal perturbations by the ohmic losses. Let $\varphi(x)$ be the static solution of (23), which coincides with one of the solutions of (1). We consider small deviations from the static solution

$$\varphi(x,t)=\varphi(x)+\Psi(x,t),\quad |\Psi(x,t)|\ll 1. \tag{24}$$

Substituting (24) in (23) and linearizing the equation, we obtain for the Fourier component of $\Psi=\psi(x)e^{\omega t}$ the equation

$$d^2\psi/dx^2-\cos\varphi(x)\psi=E\psi,\quad E=\omega^2+\beta\omega. \tag{25}$$

We assume that the solution $\varphi(x,t)$ must satisfy the boundary conditions (3). Since the static function $\varphi(x)$ satisfies this requirement, the function $\psi(x)$ should satisfy the zero boundary conditions:

$$\left.\frac{d\psi}{dx}\right|_{x=0}=\left.\frac{d\psi}{dx}\right|_{x=L}=0. \tag{26}$$

From (25), subject to the condition (26), we can obtain the spectrum of the eigenvalues E at which the problem has nontrivial solutions. Knowing the eigenvalue E, we can easily find the growth rates that determine the evolution of the solution with time:

$$\omega_{\pm}=-{}^1/_2\beta\pm[{}^1/_4\beta^2+E]^{1/2}. \tag{27}$$

It is clear therefore at $E>0$ there must exist a growing solution at the form $\psi\exp(\omega_+ t)$, $\omega_+>0$; at $E<0$ there are no growing solutions. Thus, if all the eigenvalues E are negative, then the static solution $\varphi(x)$ is stable, but for positive E the solution $\varphi(x)$ is unstable. [We note incidentally that the stability or instability of the solution is determined only by the sign of E and does not depend on the value of β in (23). All that depends on β is the growth rate (27).] Thus, an investigation of the stability of the solutions reduces to a determination of the spectrum of the eigenvalues of (25).

In the general case, as already mentioned, the solution $\varphi(x)$ of Eq. (1) is expressed in terms of elliptic Jacobi functions. The solutions of (25) are expressed then in terms of Lamé functions (see Refs. 9 and 10). However, it is difficult to obtain readily the spectrum of the eigenvalues in this case. In the case of strong fields $H_e\gg 1$ we can use in place of $\cos\varphi(x)$ in (25) the function $\cos(\varphi_0+H_0x)$ [see (19)]. In this case the solutions of (25) simplify and the spectrum E can be obtained in explicit form.

Indeed, we write in place of (25) the equation

$$d^2\Psi/dx^2-\cos(\varphi_0+H_0x)\psi=E\psi \tag{28}$$

and seek for it a solution that satisfies the boundary conditions

$$\psi|_{x=0}=1,\quad \left.\frac{d\psi}{dx}\right|_{x=0}=0 \tag{29}$$

(in place of unity we can use here an arbitrary constant C).

The change of variable $\varphi_0+H_0x=z$ reduces the system (28) and (29) to the form

$$\frac{d^2\psi}{dz^2}-\frac{\cos z+E}{H_0^2}\psi=0,\qquad \left.\frac{d\psi}{dz}\right|_{z=\varphi_0}=0,\quad \psi|_{z=\varphi_0}=1. \tag{30}$$

Using the inequality $H_0\gg 1$, we can easily obtain by successive approximations a solution of the system (30) in the form

$$\psi(z)=1+\frac{1}{H_0^2}\left\{\frac{Ez^2}{2}-(\sin\varphi_0+E\varphi_0)z+E\frac{\varphi_0^2}{2}+\varphi_0\sin\varphi_0+\cos\varphi_0-\cos z\right\}.$$

We stipulate, in accord with (26) that $d\psi/dx|_{x=L}=0$, i.e., that $d\psi/dz_{z=z_0}=0$, where $z_0=\varphi_0+LH_0$. This requirement makes it possible to find the spectrum of the eigenvalues:

$$E=(\sin\varphi_0-\sin z_0)/(z_0-\varphi_0)$$

or

$$E=-\frac{1}{\varphi}\sin\phi\cos(\phi+\varphi_0),\qquad \phi=H_eL/2. \tag{31}$$

Substituting in (31) the expression $\varphi(0)=\pm 2\xi_N$ from (13), we get

$$E=(-)^{n+1}\frac{\sin\phi}{\phi}\sigma_N\cos a(\phi), \tag{32}$$

where N is the number of the investigated solution, $\sigma_N=+1$ for $N=0,1,3,\ldots$ and $\sigma_N=-1$ for $N=0',2,3',\ldots$ (the appearance of the factor $\sigma_N=\pm 1$ in (32) is due to the additional term $\pi/2$ in formulas (13), $n=0,1,2,\ldots$ are the numbers of the curves on Fig. 2a, while the function $a(\phi)$ is defined in (14).

On the basis of the form of formula (32), we easily find, for example, that $E<0$ for $n=0$ for solutions with numbers $N=0,1,3$ (i.e., these solutions are stable), while $E>0$ for solutions with numbers $N=0',2,3'$ (i.e., these solutions are unstable). The stable and unstable branches of the solutions are shown in Fig. 2c by thick and thin lines, respectively.[2)] All other solutions at $n\neq 0$ are similarly classified (see Fig. 2a).

We note that it is possible to conclude that any solution $\varphi_N(x)$ obtained on the basis of the linearized equation (28) is stable, can be verified by a direct numerical calculation of the partial differential equation (23). It is seen here that the unstable solutions are indeed transformed in the course of time and go over into the corresponding stable solutions (see, e.g., Refs. 5–7, which show examples of the evolution of the solutions with time). It is possible that the unstable solutions can manifest themselves in nonstationary problems or in the dynamic model of dislocations, which is similar in its mathematical formulation.[11-14] We are therefore justified in calling attention to the existence of unstable solutions.

5. MAXIMUM CURRENT AND AVERAGE FIELD IN THE JUNCTION

We now consider the question of the value of the maximum current that can flow through a tunnel junction of width L in a given external field H_e. In the general case this relation is highly nonlinear (see, e.g., the numerical calculations of Owen and Scalapino,[3] and also the survey of the experimental work in Ref. 2). In the case of a strong external field, $H_e\gg 1$, this dependence can be obtained in analytic forms for a barrier of finite width.

As seen from Fig. 2, when the parameter $p=H_eH_I$ increases, the integral curves contract to the point $\phi=\pi(n+\frac{1}{2})$. Consequently, at a given position of the line $J=\phi$ (i.e., at given L and H_e) the maximum current $I_{\max}=2H_{I_{\max}}$ at which a static solution of the problem is still possible, is determined by the condition [see (15), (16)]

$$\phi=J_{4n}(\xi_c)=\pi n+\arcsin H_eH_I \tag{33}$$

At $\tilde\phi=\phi-n\pi<\pi/2$ (the minimum points of the J_{4n} curves) or by the condition

$$\phi=J_{4n+3}(\pi-\xi_c)=\pi(n+1)-\arcsin H_eH_I \tag{34}$$

at $\tilde\phi=\phi-n\pi>\pi/2$ (the maximum points of the curves J_{4n+3}). From this we get

$$I_{max}^{(4n)}/L=\sin\tilde\phi/\phi,\quad 0\leqslant\tilde\phi\leqslant\pi/2,\qquad I_{max}^{(4n+3)}/L=\sin\tilde\phi/\phi,\quad \pi/2\leqslant\tilde\phi\leqslant\pi. \tag{35}$$

With increasing ϕ, the quantity $\tilde{\phi}=\phi-n\pi$, remains all the time in the interval $0\leqslant\tilde{\phi}\leqslant\pi$, while $\sin\tilde{\phi}\geqslant 0$. It is clear that expressions (35) can be rewritten in the equivalent form

$$I_{max}/L=|\sin\phi|/\phi, \quad \phi=H_eL/2. \tag{36}$$

Formula (36) is usually cited in the books on the Josephson effect[1,2] with reference to some analogy with the formula for Fraunhofer diffraction in optics. This formula was first proposed in Ref. 11 on the basis of simple physical considerations and was found to be in good agreement with experimental results[2,11,12] for junctions of small width, $L\ll 1$. It was shown above this formulas remain in force also for junctions of finite width, but to justify it we must go outside the framework of the linear approximation.

Besides the curve for the maximum current, it is of definite interest to obtain the plot of the termination points of the solutions number 1, 5, ... As is clear from Fig. 2c, the corresponding termination points of the solutions are defined by the equations

$$\begin{aligned}&\phi=J_{4n+1}(\xi=0), \quad \tilde{\phi}=\phi-n\pi<\pi/2,\\ &\phi=J_{4n+1}(\xi=\xi_*), \quad \tilde{\phi}=\phi-n\pi>\pi/2.\end{aligned} \tag{37}$$

Using (13) and (17) we easily get

$$\begin{aligned}&J_{4n+1}(\xi=0)=\pi n+\arcsin(H_eH_1)^{1/2},\\ &J_{4n+1}(\xi=\xi_*)=\pi(n+1)-\arcsin(H_eH_1)^{1/2},\end{aligned}$$

and as a result Eq. (37) yields the equation for the termination line of the solutions φ_{4n+1}:

$$\begin{aligned}&I_{max}^{(4n+1)}/L=\sin^2\tilde{\phi}/\phi, \quad 0\leqslant\tilde{\phi}\leqslant\pi/2,\\ &I_{max}^{(4n+1)}/L=\sin^2\tilde{\phi}/\phi, \quad \pi/2\leqslant\tilde{\phi}\leqslant\pi.\end{aligned} \tag{38}$$

The curves for the maximum current (35) and (38) for different solutions are shown in Fig. 7. We note that our analysis is limited to the case of strong fields,[3)] $H_e\leqslant 1$, and therefore the region $H_e\leqslant 1$ in Fig. 7 is in fact described correctly by formulas (35) and

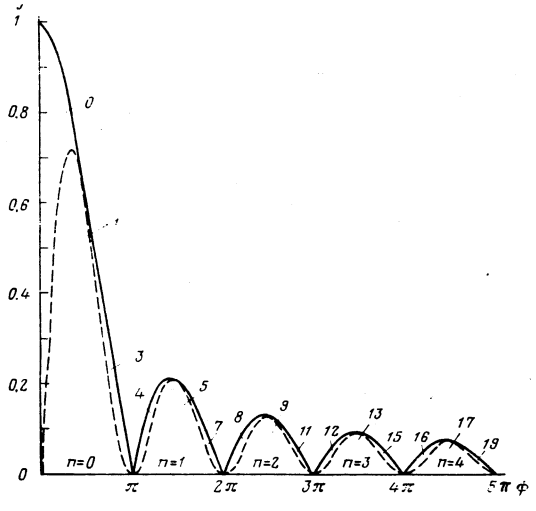

FIG. 7. Maximum current $j=2H_I/L$ as a function of the applied field $\phi=H_eL/2$. Solid line—stationarity limit (35). The dashed curve bounds the region of the existence of solutions φ_{4n+1} (38). The numbers mark the regions of the existence of solutions numbered as in Fig. 2a.

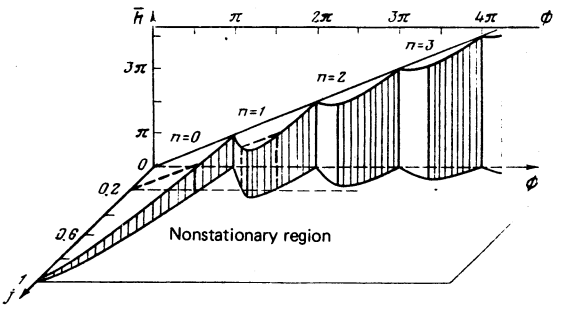

FIG. 8. Average field $\bar{h}=L\bar{H}/2$ in the junction as a function of the applied field $\phi=H_eL/2$ and of the total current $j=2H_I/L$. The dashed lines show the section of the $\bar{h}$ surface at $j=0$ and 2. The region of the parameters at which the nonstationary Josephson effect is realized is indicated.

(38) only if $L\leqslant 1$. For finite values $L>1$ and $H_e\sim 1$, as shown by numerical calculations,[3] the field dependence is more complicated, and the ascending and descending sections of the curves of the maximum current are described by nonsymmetrical relations, in contrast to the symmetrical formulas (35) and (38). In this case the curves in Fig. 7 begin to overlap and sections of hysteresis origin appear. Our analysis shows that with increasing field the strong linear dependence[3] degenerates, and the maximum-current curves must end up with the simple relation (35), (38) even in the case of broad junctions ($L\geqslant 1$).

Some interest attaches also to the dependence of the average field $\bar{H}$ in the junction through which the transport current flows on the applied external field H_e, i.e., to finding the magnetization curve of a weak current-carrying superconductor. We have

$$\bar{H}=\frac{1}{L}\int_0^L\frac{d\varphi}{dx}dx=\frac{\varphi(L)-\varphi(0)}{L}, \quad \varphi(L)=\pm 2A+2\pi n, \tag{39}$$

where A is defined in (9). Using the explicit dependence $\varphi(0)=\pm 2\xi_N$ on the field $\phi=H_eL/2$, obtained in (13) and (14), and also the trigonometrical identity (which is valid in the region of the admissible values of p and ϕ)

$$\arcsin[p+\sin^2\xi(\phi)]^{1/2}+\xi(\phi)\equiv\phi, \quad \xi(\phi)=\frac{\phi}{2}-\frac{1}{2}\arcsin\frac{p}{\sin\phi},$$

we readily obtain

$$\bar{H}(\phi)=\phi, \quad H_e\gg 1, \quad \phi=H_eL/2, \tag{40}$$

where the function $\bar{H}(\phi)$ is defined in those regions where the solutions $\varphi_N(x)$ of the problem exist (see Fig. 8). Thus, the magnetization curve of a weak superconductor with current in a strong field is made up of a set of linear segments. (As seen from the approximate solution (19), when the nonlinear corrections are taken into account these linear segments become somewhat corrugated.)

In conclusion, we point out a peculiear "geometric resonance" in a system of Josephson junctions of different widths situated in an identical external field H_e. As is clear from Fig. 3, in the absence of a current, some static vortex structure is realized in a barrier of arbitrary width. When a weak current is turned on, static solutions vanish first for junctions of width $2\pi n/H_e$. This means that junctions with widths $2\pi/H_e$,

$4\pi/H_e, \ldots$ should simultaneously go over into a nonstationary regime. On the other hand, junctions of width $\pi/H_e, 3\pi/H_e, \ldots$ are the last to become unstable and can withstand a maximum current $I = 2/H_e$. This circumstance can probably be used for a width calibration of Josephson junctions.

[1)]All the solutions of Eq. (1) can be expressed in terms of Jacobi elliptic functions. The different types of solutions referred to here are characterized by different numbers of extremal points in the interval $0 < x < L$ (different numbers of zeros of the current, see Sec. 3), and are determined by different initial values.

[2)]The onset of a topological factor $\sigma_N = \pm 1$ for the entire aggregate of the stable (or unstable) solutions is evidence that, from the point of view of stability, we are dealing not with different types of solutions, but with two branches—stable and unstable (see Fig. 2c). The subdivision, for example, of the stable branch into solutions of the type 0, 1, 3 is meaningful when it comes to classifying the solutions in accordance with the character of their coordinate dependences (in accordance with the number of extremal points, see Sec. 3).

[3)]The condition $H_e \gg 1$ means in dimensional units $H_e \gg H_J \sim 1G$, i.e., formulas (35) and (38) describe in fact a rather wide field interval.

[1]I. O. Kulik and I. K. Yanson, Effekt Dzhosefsona v sverkhprovodyashchikh tunnel'nykh strukturakh (Josephson Effect in Superconducting Tunnel Structures), Nauka, 1970.
[2]L. Solymar, Superconductive Tunneling and Applications, Halsted, 1972.
[3]C. S. Owen and D. J. Scalapino, Phys. Rev. **164**, 538 (1967).
[4]G. F. Zharkov, Zh. Eksp. Teor. Fiz. **71**, 1951 (1976) [Sov. Phys. JETP **44**, 1023 (1976)].
[5]G. F. Zharkov and S. A. Vasenko, Zh. Eksp. Teor. Fiz. **74**, 665 (1978) [Sov. Phys. JETP **47**, 350 (1978)].
[6]G. F. Zharkov and A. D. Zankin, Fiz. Nizk. Temp. **4**, 586 (1978) [Sov. J. Low Temp. Phys. **4**, 283 (1978)].
[7]S. A. Vasenko and G. Zharkov, Zh. Eksp. Teor. Fiz. **75**, 180 (1978) [Sov. Phys. JETP **48**, 89 (1978)].
[8]A. A. Andronov, A. A. Vitt, and S. E. Khaikin, Teoriya kolebanii (Theory of Oscillations), Fizmatgiz, 1959. [Addison-Wesley, 1966].
[9]P. Lebwohl and M. J. Stephen, Phys. Rev. **163**, 376 (1967).
[10]B. Sutherland, Phys. Rev. A **8**, 2514 (1973).
[11]J. Frenkel and T. Kontorova, Phys. Z Sowjetunion **13**, 1 (1938).
[12]F. C. Frank and J. H. Van der Merwe, Proc. R. Soc. London **198**, 203, 216 (1949).
[13]A. Seeger and A. Kochendorfer, Z. Phys. **127**, 531 (1950); 130, 321 (1951).
[14]A. Seeger, H. Dorth, and A. Kochendorfer, Z. Phys. **134**, 173 (1953).
[15]R. C. Jaklevic, J. Lambe, A. H. Silver, and J. E. Mercerau, Phys. Rev. Lett. **12**, 159 (1964).
[16]J. M. Rowell, Phys. Rev. Lett. **11**, 200 (1963).

Translated by J. G. Adashko

Accidental degeneracy of self-localized solutions of the Landau-Lifshitz equations

V. M. Eleonskiĭ, N. N. Kirova, and N. E. Kulagin

(Submitted 26 May 1978)
Zh. Eksp. Teor. Fiz. **75**, 2210–2219 (December 1978)

It is shown that the self-localized solutions of the Landau-Lifshitz equations for a uniaxial ferromagnet with anisotropy energy $K \sin^2\theta$ are degenerate. Specifically, for an arbitrary velocity of an isolated magnetic-moment wave there exists a continuous set of self-localized solutions, which correspond to a definite type of magnetic solitons. If one goes over to a more general expression for the uniaxial-anisotropy energy, such as $K(\sin^2\theta + \beta \sin^4\theta)$ $(\nu > 0)$, or if one allows for an external field, the accidental degeneracy is removed; this leads to disintegration of the continous set of solutions of the soliton type and to formation of a countable set of self-localized solutions of the isolated-wave type, with a definite internal structure.

PACS numbers: 75.10.Jm, 75.30.Gw

1. Investigations of nonlinear magnetic-moment waves, carried out both by the method of analytic continuation of the spin-wave spectrum into the region of complex wave vectors[1] and by direct analysis of the asymptotic behavior of the magnetic-moment distribution in the region of establishment of a homogeneous state,[2] have made it possible to determine characteristic limiting velocities of "slow" and "fast" nonlinear waves, and also to separate the regions of existence of definite types of stationary-profile waves; for example, the moving-domain-wall type or the isolated-wave type (magnetic soliton).

0038-5646/78/1201113-06$02.40